RESEARCH ARTICLE

Lactoferrin during lactation protects the immature hypoxic-ischemic rat brain

Yohan van de Looij[1,2,a], Vanessa Ginet[1,a], Alexandra Chatagner[1], Audrey Toulotte[1], Emmanuel Somm[1], Petra S. Hüppi[1] & Stéphane V. Sizonenko[1]

[1]Division of Child Development and Growth, Department of Pediatrics, University of Geneva, Geneva, Switzerland
[2]Laboratory for Functional and Metabolic Imaging (LIFMET), Ecole Polytechnique Fédérale de Lausanne (EPFL), Lausanne, Switzerland

Correspondence
Yohan van de Looij, Laboratory for Functional and Metabolic Imaging, Ecole Polytechnique Fédérale de Lausanne, CH F1 602 - Station 6, 1015 Lausanne, Switzerland. Tel: (+41) 21 693 79 38; Fax: (+41) 21 693 79 60; E-mail: yohan.vandelooij@epfl.ch

[a]First two authors contributed equally.

Abstract

Objective: Lactoferrin (Lf) is an iron-binding glycoprotein secreted in maternal milk presenting anti-inflammatory and antioxidant properties. It shows efficient absorption into the brain from nutritional source. Brain injury frequently resulting from cerebral hypoxia-ischemia (HI) has a high incidence in premature infants with ensuing neurodevelopmental disabilities. We investigated the neuroprotective effect of maternal nutritional supplementation with Lf during lactation in a rat model of preterm HI brain injury using magnetic resonance imaging (MRI), brain gene, and protein expression. **Methods**: Moderate brain HI was induced using unilateral common carotid artery occlusion combined with hypoxia (6%, 30 min) in the postnatal day 3 (P3) rat brain (24–28 weeks human equivalent). High-field multimodal MRI techniques were used to investigate the effect of maternal Lf supplementation through lactation. Expression of cytokine coding genes (TNF-α and IL-6), the prosurvival/antiapoptotic AKT protein and caspase-3 activation were also analyzed in the acute phase after HI. **Results**: MRI analysis demonstrated reduced cortical injury in Lf rats few hours post-HI and in long-term outcome (P25). Lf reduced HI-induced modifications of the cortical metabolism and altered white matter microstructure was recovered in Lf-supplemented rats at P25. Lf supplementation significantly decreased brain TNF-α and IL-6 gene transcription, increased phosphorylated AKT levels and reduced activation of caspase-3 at 24 h post-injury. **Interpretation**: Lf given through lactation to rat pups with cerebral HI injury shows neuroprotective effects on brain metabolism, and cerebral gray and white matter recovery. This nutritional intervention may be of high interest for the clinical field of preterm brain neuroprotection.

Introduction

Breast milk is considered as the ideal nutrient for newborns, given the clinical evidence for its benefits.[1] Several of its components have been shown to be positively correlated to cerebral development[2] including lactoferrin (Lf). Lf is an iron-binding glycoprotein[3] with multiple biological functions (iron absorption, anti-inflammatory, immunomodulator, antioxidant, host defense mechanism, anticarcinogenicity).[4–9] It is produced by exocrine glands and released in mucosal secretions including at a high level in colostrum and maternal milk.[10] It has been reported recently that Lf reduces the incidence of late-onset sepsis in preterm infants[11] and prevents necrotizing enterocolitis in preclinical models.[8,12] Moreover, it delayed inflammation-induced preterm delivery in mice and rabbits[13,14] and possibly women.[15] Recently, we were able to show that prenatal Lf in a rat model of intrauterine growth restriction protected the brains of the offspring.[16]

In rodents after oral administration, Lf is rapidly transferred from the intestine to blood and into various organs including the brain where Lf receptors are expressed in neurons and brain endothelial cells.[17,18] Moreover, in

view of its high brain uptake capacity it has been used as a vector to deliver neuroprotective agents into the brain.[19–21] Lf is also overexpressed in the brain in association with age related neurodegenerative disorders[22] such as Parkinson's disease[23,24] or Alzheimer's[24,25] where it may represent a protective mechanism against ongoing neuronal death.[25,26]

In extremely preterm infants (born between 24 and 28 weeks of gestation), encephalopathy of prematurity, including periventricular leukomalacia, is the most common form of brain injury with severe long-term neurodevelopmental disabilities.[27] Two major etiologies are generally involved: cerebral ischemia/reperfusion and bacterial infection/inflammation in the mother and/or fetus.[27]

Cerebral hypoxia-ischemia (HI) in the 3-day-old (P3) rat is commonly used as an animal model of preterm brain injury with altered cortical development and white matter integrity.[28–31] We have shown with [1]H-Magnetic Resonance Spectroscopy (^{1}H-MRS) at ultra-high magnetic field that specific acute and long-term changes in the "neurochemical profile" are observed in this model.[31] Further diffusion tensor imaging (DTI) allows a precise assessment of brain microstructure and has been used to delineate white matter microstructural damage and recovery.[28,32–36] Phase contrast imaging (PCI), a technique based on the sensitivity to differences in resonance frequency in the phase of gradient-echo MR images with excellent contrast between white and gray matter,[37] has recently been used to assess the myelination process in the developing mouse brain[38] and microstructural effects of axonal density have been shown by phase contrast imaging,[39] making PCI a powerful tool for assessing white matter microstructure.

Currently there is paucity of treatment to reduce early preterm brain injury and to support normal cerebral development. As Lf is a physiological compound with several beneficial biological effects that have the potential to reduce brain damage after HI injury in the preterm brain, we hypothesized that maternal nutritional supplementation with Lf could be effective in early brain injury. Further it is a commercially available food complement reasonably priced with no or very rare adverse effects or intolerances described in clinical studies.[15,40–42] For all these reasons, Lf supplementation could represent a promising safe and affordable (i.e., in emerging countries) approach for prevention and improvement of the clinical outcome for premature newborns with brain injury and altered development. In this study, a multimodal MRI protocol combined with biochemical analysis was used to assess the long-term neuroprotective effect of maternal Lf supplementation during lactation in P3 rat HI brain injury.

Materials and Methods

Animal model

The Geneva State Animal Ethics Committee and the Swiss Federal Veterinary Service approved these studies. At birth (P0), Wistar rat dams (from Geneva School of Medicine breeding) received either an Lf (Lactoferrin-NFQ; Taradon Laboratory, Tubize, Belgium) -enriched food (1 g/kg per day – Lf) or a diet strictly isocaloric to the Lf diet (Iso) (Provimi Kliba SA, Penthalaz, Switzerland) ad libitum during the whole period of lactation. Three days after birth (P3) pups from both groups (HI-Lf and HI-Iso) underwent moderate hypoxic-ischemic injury. The right carotid artery was double-cauterized and cut under isoflurane anesthesia (2.5%). After a 30 min recovery period, rat pups were exposed to hypoxia (6% O_2) at 37°C for 30 min. Sham rat pups from both groups underwent the same anesthesia to isolate the common carotid artery without cauterization and were not exposed to hypoxia.

To reduce inter- and intralitter variability, experimental design was as follows. For each experiment, Lf and Iso litters were processed in parallel. Diets supplemented in Lf or isocaloric were randomly attributed to the litters the day of birth. At P3 all the rats of the Lf and Iso litters underwent HI at the same time except for 1 or 2 rats per litter considered as Sham. The number of pups per litter was not significantly different between the two groups (7.5 ± 1.0 rats/litters in the Lf group and 6.9 ± 2.3 rats/litters in the Iso group, $P = 0.34$).

MR experiments

All MR experiments were performed the day of the HI injury (P3) and 22 days after (P25) on an actively shielded 9.4 T/31 cm magnet (Varian/Magnex) equipped with 12-cm gradient coils (400 mT/m, 120 μsec) using a quadrature transceive 17-mm surface RF coil. P3 and P22 rats were continuously anesthetized under a flow of 1.5–2% isoflurane in oxygen and their body temperature was maintained at 37 ± 0.5°C using thermoregulated water circulation. Due to the variability in the model,[29,30] we decided to exclude from this study noninjured pups at P3 from both HI-Lf and -Iso groups. As such, after screening (i.e., T_2W imaging 5 h following HI), pups that did not present any ipsilateral cortical hypersignal as sign of lesion (see below) were removed from the study, corresponding to 54.9% and 52.5% for HI-Lf and HI-Iso groups, respectively. The number of pups removed per group was not significantly different between HI-Lf and HI–Iso groups. Finally, 16 rats in the HI-Lf group (7♂ and 9♀) and 15 rats in the HI-Iso group (8♂ and 8♀), all presenting hypersignal on T_2W images as a proof of lesion,[31] were

assessed with MR at a later time point (P25). In a previous study, sham rats fed with Lf or Iso diet did not show any significant difference in MRS results,[16] so in this study they were pooled in a Sham group including 10 rats.

For measurements at P3, pups were placed in the supine position in an adapted holder. Around 5 h following HI, T_2W Fast Spin Echo (FSE) images with TR/TE = 6000/80 msec, FOV = 15 × 15 mm and matrix size = 256 × 128 were used to detect the presence of injury as well as to determine the lesion volume. The cortical injury was situated approximately from level −3.8 mm to level −0.6 mm relative to the bregma.

To study the long-term effects of Lf treatment, a multimodal MRI protocol was performed with T_2W images, ^{1}H-MRS, DTI and PI 22 days following HI. The P25 rats were fixed with bars securing their head in the holder. FSE images with the same parameters as at P3, except a FOV = 25 × 25 mm, were realized to position MRS voxel of interest (1.5 × 1.5 × 2.5 mm^3). ^{1}H-MRS acquisition and analysis protocols have been described previously.[43] Metabolites were quantified resulting in a neurochemical profile of the cortical area for each group.[43]

Before imaging experiments, first and second order shims were adjusted using FASTMAP[44] resulting in water linewidths of 16–20 Hz for a voxel of 7 × 9×8 mm^3 centered in the brain. For DTI, a semi-adiabatic double spin echo sequence was used[45] and diffusion gradients were positioned around the first 180° with the same polarity resulting in a *b*-value fixed to 1000 sec mm^{-2} (δ/Δ = 3/23 msec and *G* = 26.6 G/cm) and applied along 21 spatial directions (Icosahedral 21 directions diffusion gradient sampling scheme[46]). DT-EPI parameters were: FOV = 23 × 15 mm^2, matrix size = 128 × 64 zero filled to 256 × 168, eight slices of 0.8-mm thickness in the axial plane, eight averages with TE/TR = 42/2000 msec and four shots.

For phase imaging, gradient-echo MR images were acquired with the following parameters: TE/TR = 16/900 msec; FOV = 23 × 23 mm^2, Matrix size = 256 × 128, 18 slices of 0.4 mm thickness and eight repetitions. To remove the effect of large-scale phase shifts across the phase images, ascribed to large-scale B_0 inhomogeneities, a 2D Gaussian high-pass filter with a kernel size of 65 voxels and a width of five voxels was applied to all images.[37]

MRI data analysis

From T_2W images, volumetric measurements were performed using Anatomist/Brain Visa.[47] At P3, lesion volume (LV) as well as ipsilateral cortical volume (ICV) were measured; at P25 contralateral cortical volume (CCV) and ipsilateral cortical volume (ICV) were quantified. From the volumetric measurements we calculated the percentage of injured cortex (IC = [LV/ICV] × 100) at P3 and the percentage of cortical loss (CL = [(CCV − ICV)/CCV] × 100) at P25.[31]

Diffusivity values (MD, $D_{//}$ and $D_\perp$) and fractional anisotropy (FA) were derived from the tensor by using a homemade Matlab (Mathworks, Natick, MA) software.[34,36,43,48] Regions of interest (ROI) were delineated in the corpus callosum (CC), the external capsule (EC) and the sensorimotor cortex (SCx) at different image-planes of the brain. DTI-derived parameters were averaged in these different ROIs (MD, $D_{//}$, $D_\perp$, and FA).[34,36,43,48] Free software, MedInria DTI track (http://www.sop.inria.fr/asclepios/software/MedINRIA/), was used for the computation and the display of the principal eigenvectors (i.e., the vector corresponding to the principal diffusion direction). Phase contrast was assessed in two white matter regions: CC and EC, by calculating the frequency shift between phases in the ROI and in the adjacent gray matter.[37,38]

Bovine lactoferrin dosage

Four days after birth milk clots were removed from the stomach of 10 rat pups and their blood was collected. Blood samples were centrifuged and the resulting serum was carefully removed. Serum and milk were stored at −80°C. Milk clots (500 mg) were diluted in 1 ml of RIPA buffer (9806S ; Cell Signaling Technology, Beverly, MA, USA) containing a protease inhibitor cocktail (11873580001; Roche, Basel, Switzerland). Bovine Lf was measured using a CircuLex Bovine Lactoferrin ELISA Kit (CY-8098; Cyclex, Nagano, Japan) according to the manufacturer's instructions. A final dilution of 8 and 2 was applied for milk and serum samples, respectively.

Immunoblotting and quantitative real-time PCR

Four independent HI experiments were performed and a total of 12 Sham-Iso, 15 HI-Iso, 18 HI-Lf and 11 Sham-Lf rats were analyzed for each biochemical study. Twenty-four hours after the insult brains were dissected out in PBS containing 1 mmol/L $MgCl_2$ on ice. The ipsilateral cortex were dissected, frozen in liquid nitrogen and stored at −80°C. Total RNA and proteins were extracted with PrepEase RNA/Protein Spin Kit (78871 1 KT; Affymetrix, Santa Clara, CA, USA) using the manufacturer's instructions. Proteins pellets were resuspended in RIPA buffer as for ELISA.

For immunoblotting, protein extracts were sonicated and the protein concentration was determined using a Bradford assay. Proteins (20 μg) were separated by SDS-PAGE, transferred on nitrocellulose membrane and analyzed by immunoblotting. Antibodies were diluted in a blocking solution containing 0.1% casein (C8654; Sigma-Aldrich, St. Louis, MO, USA). The following primary

antibodies were used: rabbit polyclonal anticleaved caspase-3 (#9661; Cell Signaling Technology), rabbit polyclonal anti Phospho-AKT (#9271S; Cell Signaling Technology), rabbit monoclonal anti-pan AKT (#4685; Cell Signaling Technology), rabbit polyclonal anti-fractin, (AB3150; Millipore, Millipore, Darmstadt, Germany) and mouse monoclonal anti-α-tubulin (sc-8035; Santa Cruz Biotechnology, Santa Cruz, CA, USA). After incubation with primary antibody, the following secondary antibodies were applied: polyclonal goat anti-mouse IgG conjugated with IRDye 680 (LI-COR, B70920-02) or goat anti-rabbit IgG conjugated with IRDye 800 (926-32210; LI-COR, Lincoln, NE, USA). Protein bands were visualized using the Odyssey Infrared Imaging System (LI-COR). Odyssey v1.2 software (LI-COR) was used for densitometric analysis. Optical density values were normalized with respect to tubulin and expressed as a percentage of values obtained for Sham operated rat pups (100%). These pups did not have an MRI evaluation of the lesion, and thus represented a mix in the severity of damage seen in the model. However, because GFAP is increased after HI at 24 h[49] with Lf treatment having no effect on this astrocytic activation (Iso group: 400 ± 45%; Lf group: 451 ± 54%), rat pups without GFAP increase at 24 h were removed from further analysis which represents ~16% of uninjured pups in both HI-Iso group: 3/18 (17%) and HI-Lf group: 3/20 (15%).

For quantitative RT-PCR, RNA (5 μg) was reverse transcribed to cDNA using 400 U Moloney murine leukemia virus reverse transcriptase (28025-013; Invitrogen, Carlsbad, CA, USA), 20 U recombinant RNasin (N251B; Promega, Madison WI, USA), 0.5 μg random hexamers (Microsynth, Balgach, Switzerland), 2 mmol/l dNTP (R203; Rovalab, Teltow, Gemany), and 40 mmol/l of dithiothreitol (Invitrogen). Quantitative real-time PCR was performed with the Power SYBR Green PCR Master Mix (4367659; Applied Biosystems, Carlsbad, CA, USA) and using an ABI StepOne Plus Sequence Detection System (Applera Europe, Rotkreuz Switzerland). Gene expressions were normalized using the housekeeping ribosomal gene RPS29. Results are expressed in arbitrary units (A.U). The following primers were used: for IL-6: forward 5′-ATATGTTCTCAGGGAGATCTTGGAA-3′, reverse 5′-TGCATCATCGCTGTTCATACAA-3′; for TNF-α: forward 5′-GACCCTCACACTCAGATCATCTTCT-3′ reverse 5′-TCCGCTTGGTGGTTTGCTA-3′; for RSP29: forward 5′-GCCAGGGTTCTCGCTCTTG-3′, reverse 5′-GGCACATGTTCAGCCCGTAT-3′.

Statistics

For MR data a Mann–Whitney test was used to compare values statistically between the different groups, $P < 0.05$ being considered as significant. Biochemical data were

analyzed statistically using JMP10 software. The n values were sufficiently high for a statistical power greater than 0.8. A Welch's ANOVA test (one-way ANOVA with unequal variances) followed by a post-hoc Tukey–Kramer test were used to compare the different treatments. $P < 0.05$ was considered as significant.

Results

Lactoferrin supplemented in food of dams is delivered to rat pups through lactation

On the day of birth, the rat dam received either Lf-enriched food (1 g/kg per day) or Iso ad libitum. Four days after birth, the level of Lf present in the suckling pups milk was around 0.034 ng/mg of stomach content and 21 ng/mL in serum demonstrating that bovine Lf can be supplied through lactation to the pups and reached their brains since Lf was to reported to cross the blood brain barrier.[50] No bovine Lf was found in milk and serum of pups from the Iso group.

Lactoferrin nutritional supplementation decreases acute and long-term cortical damages after HI

A few hours after HI insult, the percentage of injured cortex (%IC) corresponding to the hypersignal on T_2W images was significantly lower for the HI-Lf group (%IC = 8.6 ± 4.8%) compared to the HI-Iso group (%IC = 14.0 ± 6.7%) ($P = 0.03$) (Fig. 1A). Twenty two days later, at P25, the percentage of cortical loss (%CL) was also significantly reduced for the HI-Lf group (%CL = 6.4 ± 6.1%) compared to the HI-Iso group (%CL = 18.6 ± 10.2%) ($P = 0.0004$) (Fig. 1B). For both groups, the percentage of cortical loss at P25 was correlated with the percentage of injured cortex at P3: $P = 0.0083$, $R = 0.64$ for the HI-Lf group and $P = 0.03$, $R = 0.55$ for the HI-Iso group (Fig. 1C). Between the two groups, R-values were similar as depicted by the parallel correlation straight lines (Fig. 1C). However, the correlation straight line of the HI-Iso group was shifted rightwards and upwards compared to the HI-Lf group. In the cortex (Fig. 1D), all the diffusivity values (MD, $D_{//}$, and $D_{\perp}$) were found to be significantly lower in the HI-Iso group (MD = 7.6 ± 0.4 × 10^{-4} mm^2 s^{-1}, $D_{//}$ = 9.5 ± 0.4 × 10^{-4} mm^2 s^{-1}, $D_{\perp}$ = 6.7 ± 0.4 × 10^{-4} mm^2 s^{-1}) compared to the HI-Lf (MD = 7.9 ± 0.2 × 10^{-4} mm^2 s^{-1}, $D_{//}$ = 9.7 ± 0.2 × 10^{-4} mm^2 s^{-1}, $D_{\perp}$ = 7.0 ± 0.2 × 10^{-4} mm^2 s^{-1}) and Sham (MD = 7.9 ± 0.1 × 10^{-4} mm^2 s^{-1}, $D_{//}$ = 9.8 ± 0.2 × 10^{-4} mm^2 s^{-1}, $D_{\perp}$ = 7.0 ± 0.1 × 10^{-4} mm^2 s^{-1}) groups, whereas no difference was observed between HI-Lf and the Sham group.
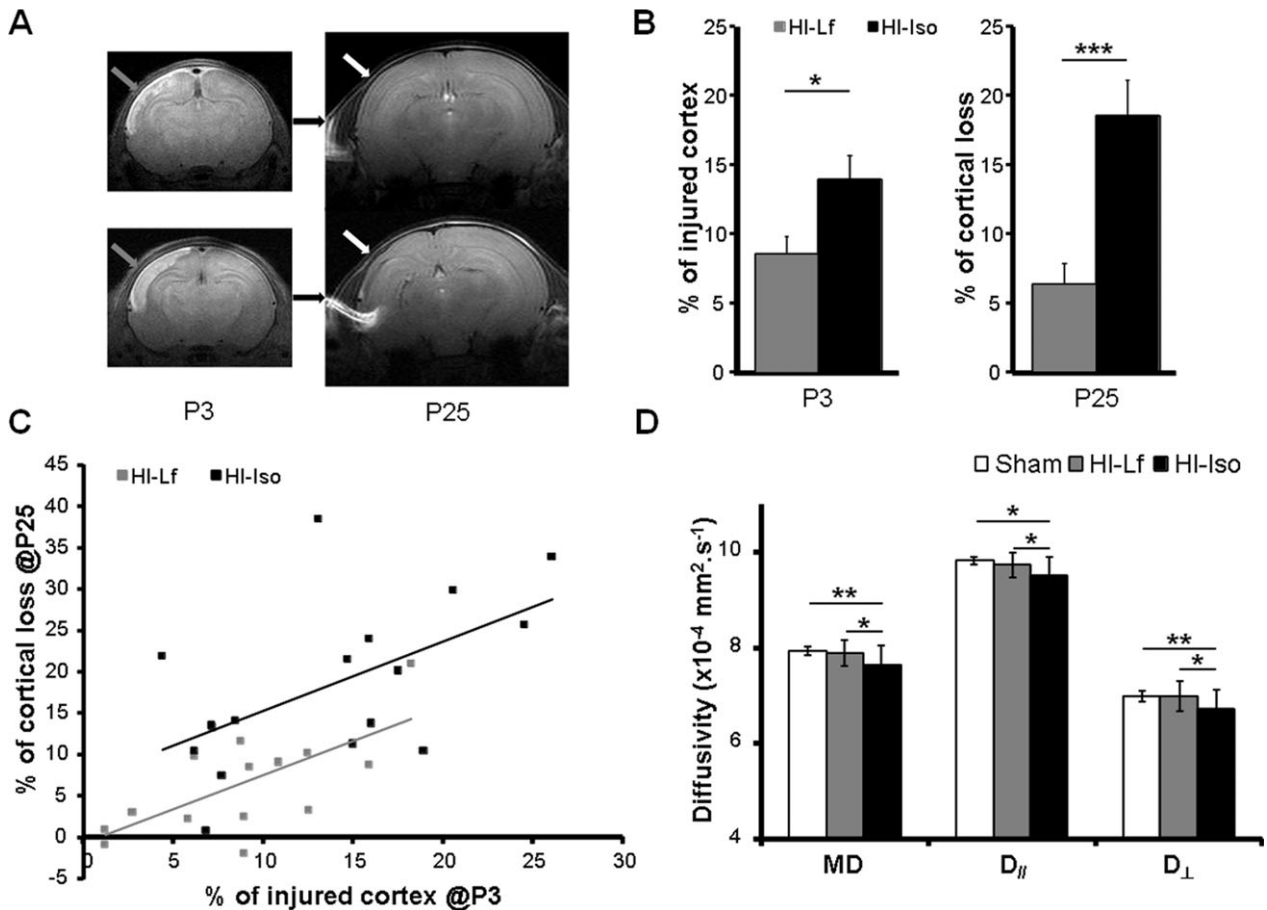
Figure 1. Lactoferrin nutritional supplementation reduces cortical damage. (A) Typical T$_2$W images of rat pups treated with lactoferrin (Lf) (upper panel) or an isocaloric diet (Iso) (lower panel) 3–6 hours (P3) (left) or 22 days (P25) (right) after HI. Cerebral edema early after HI (gray arrows) as well as cortical loss 22 days after HI (white arrows) are obvious for both groups and are smaller in Lf-treated animals. (B) Histograms of the percentage of injured cortex at P3 and of cortical loss at P25 for both groups, showing a significant reduction in cortical damage in HI-Lf animals: HI-Lf (gray) and HI-Iso (black) (*$P < 0.05$). Values are mean $\pm$ SD. (C) Correlations between the percentage of injured cortex at P3 and the percentage of cortical loss at P25 for both groups: HI-Lf (gray) and HI-Iso (black). (D) Histograms of the mean values of diffusivities (MD, D$_{//}$ and D$_\perp$) of the Sham (white), HI-Lf (gray) and HI-Iso (black) groups measured in the cortex. Values are mean $\pm$ SD, *$P < 0.05$, **$P < 0.01$, ***$P < 0.001$. HI, hypoxia-ischemia.

In terms of cortical damage, the reduction by Lf in % of injured cortex at P3 was 32% for males and 43% for females. Indeed, at P25, the % of cortical loss was reduced by 50% for males and 67% for females by Lf. We believe the volume reduction of the hyperintense signal as marker of reduced initial brain injury in the HI-Lf group results from Lf treatment. We base this assumption on the fact that our experimental procedure was designed to reduce inter- and intralitter variability, and that different levels of damage could be seen within both groups, as previously observed in this model.[31]

Cortical metabolism modifications induced by hypoxia-ischemia are reduced by lactoferrin

At P25, ^{1}H-MRS achieved very good spectral quality, as judged from water linewidth, obtained with FASTMAP

ranging from 8 to 12 Hz (Fig. 2A). Due to very thin cortical structure in the rat pup brain, MRS was performed on a very small volume of 5.6 μL placed on the ipsilateral cortex. Overall, in this study, SNR was equal on average to 23 $\pm$ 3. These consistent data were subjected to spectral analysis and absolute quantification by LCModel providing the concentration of 17 metabolites defined as the "neurochemical profile".[31] Comparison of ipsilateral HI-Iso and Sham cortex profiles (Fig. 2B) showed a significant decrease of GABA (Sham: 1.2 $\pm$ 0.3 μmol/g, HI-Iso: 0.9 $\pm$ 0.2 μmol/g), NAA, (Sham: 8.9 $\pm$ 0.3 μmol/g, HI-Iso: 8.4 $\pm$ 0.6 μmol/g) and Taurine (Sham: 8.3 $\pm$ 0.4 μmol/g, HI-Iso: 7.9 $\pm$ 0.6 μmol/g) concentrations as well as a significant increase of NAAG (Sham: 0.6 $\pm$ 0.2 μmol/g, HI-Iso: 0.8 $\pm$ 0.2 μmol/g) concentrations in the lesion area. Under Lf treatment only NAA (HI-Lf: 8.3 $\pm$ 0.6 μmol/g) concentration was
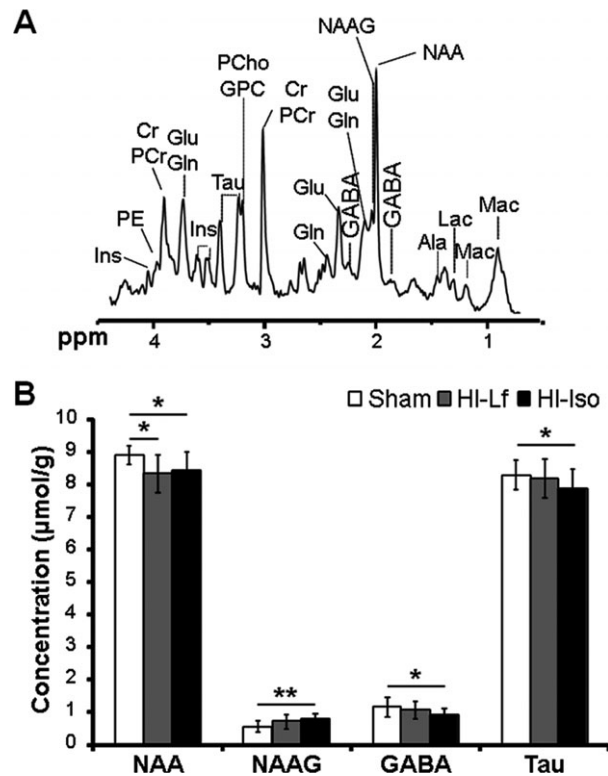
Figure 2. Lactoferrin treatment reduces cortical metabolism alterations induced by perinatal hypoxia-ischemia (HI). (A) Representative 9.4 T spectrum in the ipsilateral cortex of a rat pup treated with lactoferrin (Lf), 22 days (P25) after hypoxia-ischemia (HI). (B) Histogram of the concentrations of the metabolites which are significantly modified at P25 by HI in rat pups treated with an isocaloric diet (HI-Iso) (black) compared to Sham. The Lf-treated (HI-Lf) (gray) group present less change, showing only a decreased NAA concentration compared to the sham group. Values are mean ± SD, *$P < 0.05$, **$P < 0.01$, ***$P < 0.001$. Mac, macromolecules; Asc, ascorbate; bhB, beta-hydroxybutyrate; PCho, phosphorylcholine; Cr, creatine; PCr, phosphocreatine; GABA, γ-aminobutyric acid; Glc, glucose; Glu, glutamate; Gln, glutamine, myo-Ins, myo-inositol; Lac, lactate; NAA, N-acetylaspartate; NAAG, N-acetylaspartylglutamate; PCr, phosphocreatine; PE, phosphoethanolamine; Tau, taurine.

significantly lower in the injured cortical area compared to Sham animals, whereas GABA, Taurine, and NAAG values were restored in the HI-Lf group.

Lactoferrin treatment mitigates white matter abnormalities detectable by DTI-derived parameters

Direction-encoded color maps showed high-quality maps with high signal-to-noise ratio leading to an accurate quantification of DTI-derived parameters (Fig. 3A, F, and K). In the EC, HI at P3 led to a reduction in all the diffusivity values at P25 (Fig. 3P) in the HI-Iso group (MD = 8.5 ± 0.5 × 10^{-4} mm^2 s^{-1}, D$_{//}$ = 12.1 ±

0.7 × 10^{-4} mm^2 s^{-1}, D$_\perp$ = 6.7 ± 0.4 × 10^{-4} mm^2 s^{-1}) compared to the Sham group (MD = 8.8 ± 0.2 × 10^{-4} mm^2 s^{-1}, D$_{//}$ = 12.6 ± 0.7 × 10^{-4} mm^2 s^{-1}, D$_\perp$ = 6.8 ± 0.2 × 10^{-4} mm^2 s^{-1}) and to the HI-Lf group (MD = 8.9 ± 0.4 × 10^{-4} mm^2 s^{-1}, D$_{//}$ = 12.7 ± 0.7 × 10^{-4} mm^2 s^{-1}, D$_\perp$ = 7.0 ± 0.4 × 10^{-4} mm^2 s^{-1}). Indeed, fractional anisotropy (FA) values (Fig. 3Q) were significantly lower in the HI-Iso group (FA = 0.41 ± 0.02) than in the Sham group, (FA = 0.44 ± 0.03) whereas no difference was observed between HI-Lf (FA = 0.42 ± 0.03) and Sham rats. EC alterations in HI-Iso rats can also be observed in the principal eigenvectors map at P25, with an altered track in the HI-Iso map, (Fig. 3L) whereas the track looks similar to Sham (Fig. 3B) in the HI-Lf map (Fig. 3G). In the corpus callosum (Fig. 3R and S) a similar trend was found in the HI-Iso (MD = 8.5 ± 0.4 × 10^{-4} mm^2 s^{-1}, D$_{//}$ = 13.5 ± 0.6 × 10^{-4} mm^2 s^{-1}, D$_\perp$ = 6.0 ± 0.5 × 10^{-4} mm^2 s^{-1} and FA = 0.50 ± 0.03) and HI-Lf (MD = 8.9 ± 0.2 × 10^{-4} mm^2 s^{-1}, D$_{//}$ = 14.1 ± 0.8 × 10^{-4} mm^2 s^{-1}, D$_\perp$ = 6.4 ± 0.3 × 10^{-4} mm^2 s^{-1} and FA = 0.49 ± 0.04) groups with significant reduction of diffusivity values and FA compared to the Sham group (MD = 9.0 ± 0.3 × 10^{-4} mm^2 s^{-1}, D$_{//}$ = 14.9 ± 0.4 × 10^{-4} mm^2 s^{-1}, D$_\perp$ = 6.1 ± 0.4 × 10^{-4} mm^2 s^{-1} and FA = 0.54 ± 0.02) except for the radial diffusivity which was slightly increased in the HI-Lf group.

Phase contrast was analyzed in the three different groups at P25 (Fig. 3T). High standard deviation in the data was observed. Nevertheless, the frequency shift between EC and adjacent gray matter of the HI-Lf and Sham groups tended to be similar and lower that of the HI-Iso group. This difference can also be observed in phase images (Fig. 3D, I, and N) and especially in EC zoom (Fig. 3E, J, and O) with similar contrast in Sham (Fig. 3E) and HI-Lf (Fig. 3J) maps, whereas the contrast was more pronounced in HI-Iso maps (Fig. 3O) matching well frequency shifts in the different groups (Fig. 3T). In the corpus callosum, as for the DTI results, frequency shifts of both HI-Lf and HI-Iso groups were different from Sham.

Expression of IL-6 and TNF-α genes is decreased by lactoferrin treatment

The effect of Lf treatment on the transcription of two different pro-inflammatory cytokines (TNF-α and IL-6) was investigated by quantitative RT-PCR during the acute phase (Fig. 4). Twenty-four hours after HI, the mRNA expressions of both the cytokines were increased in the cortex (HI-Iso, TNF-α: 6.03 ± 0.95; IL-6: 7.95 ± 0.79). Thus, nutritional supplementation with lactoferrin significantly reduced TNF-α and IL-6 (HI-Lf, 4.57 ± 0.59 and 3.75 ± 0.42, respectively) gene transcription.
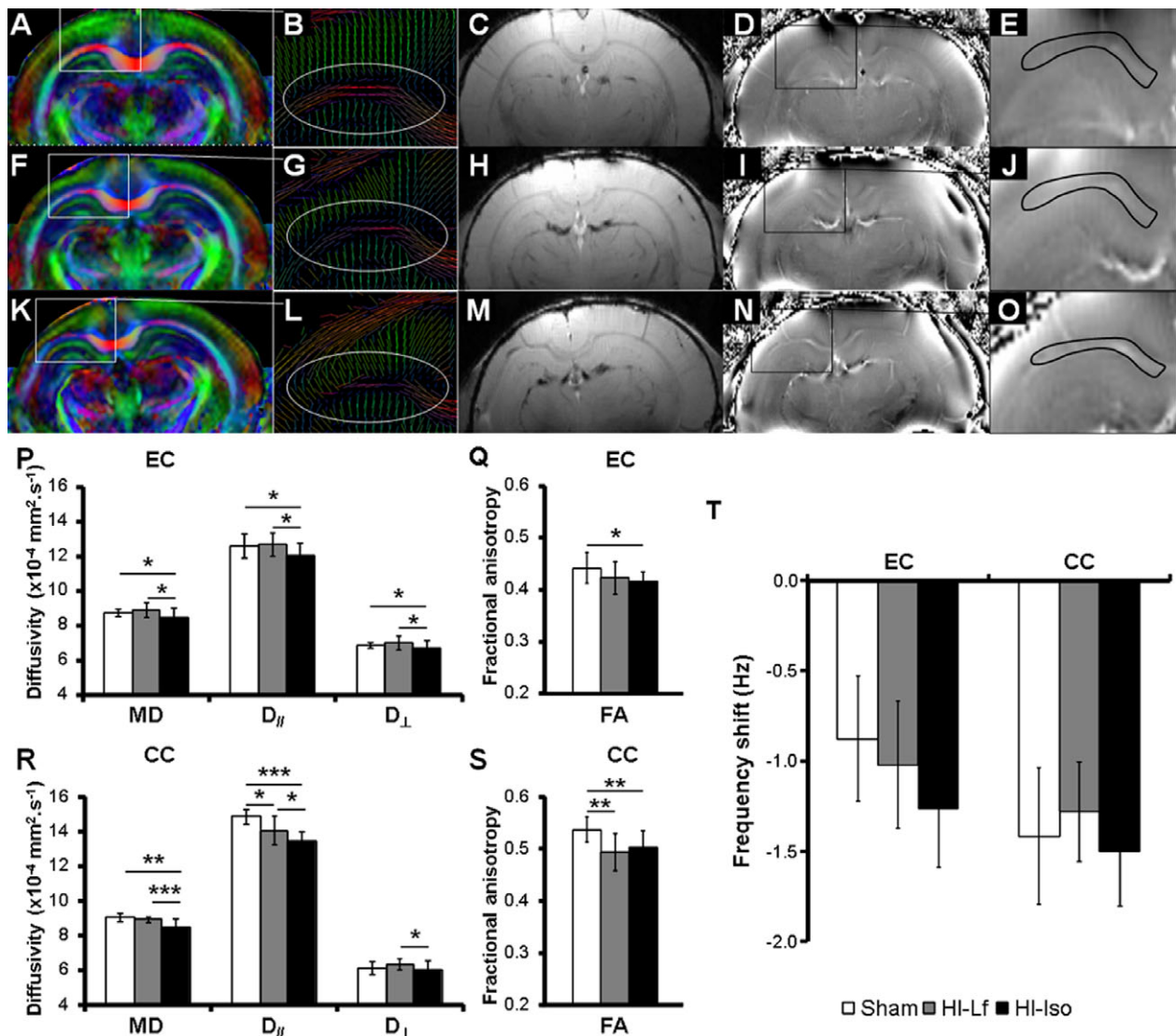
Figure 3. Protective effect of lactoferrin on white matter damage revealed by high-field DTI and phase contrast. Typical images of Sham (A–E), HI-Lf (F–J) or HI-Iso (K–O) rats 22 days (P25) after P3 cerebral hypoxia-ischemia showing white matter damage in direction-encoded color maps (A, F, and K) and altered track of the eigenvectors in the HI-Iso group in zoom on the EC (circles in B, G, and L). T_2*W images (C, H, and M) revealing less severe cortical lesions in an HI-Lf rat. Phase contrast images (D, I, and N) and zoom on the EC (E, J, and O) illustrating the differences in contrast on phase images between the Sham, HI-Lf and HI-Iso groups (E, J, and O, respectively; contrast between black delineated zone in EC and adjacent gray matter). Histograms of the mean diffusion tensor imaging-derived parameters values: diffusivity values MD, $D_{//}$ and $D_{\perp}$ (P, R) and fractional anisotropy (FA) (Q, S) of the Sham, HI-Lf and HI-Iso groups measured in the EC (P, Q) and the CC (R, S). Values are mean ± SD, *$P < 0.05$, **$P < 0.01$, ***$P < 0.001$. Histogram of the mean values of frequency shift over the EC and corpus callosum for the Sham, HI-Lf and HI-Iso groups (T, values are mean ± SEM). HI, hypoxia-ischemia.

Lactoferrin treatment reduced AKT dephosphorylation and activation of caspase-3

Caspase-dependent apoptosis is involved in neuronal damage following cerebral perinatal HI. The effect of Lf on the activation of caspase-3 was studied 24 h after HI (Fig. 5). In the cortex of HI-Lf animals, reduced caspase-3 activa-

tion was measured (1638 ± 188%) compared to HI-Iso rats (HI: 2413 ± 247%) (Fig. 5A). Even though caspase-3 activation was not abolished by Lf treatment, its positive effect on the caspase-3-dependent apoptotic pathway was confirmed by a reduced production of fractin, the caspase-cleaved fragment of actin (HI-Iso: 810 ± 70%, HI-Lf: 561 ± 47%). The signaling pathway of AKT (also known as Protein Kinase B) plays an antiapoptotic role by regulat-
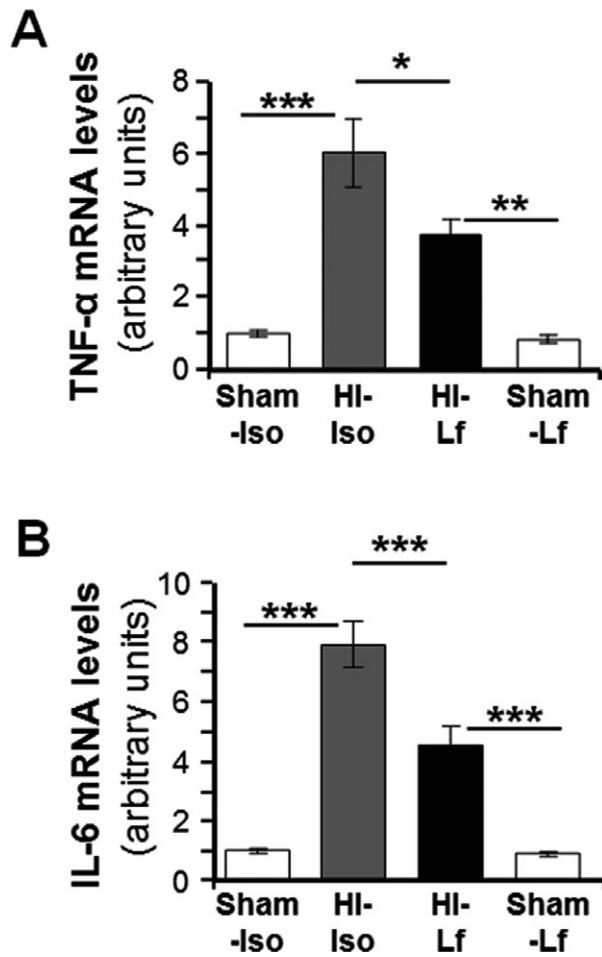
Figure 4. Nutritional supplementation with lactoferrin decreased TNF-α and IL-6 genes transcription. Quantitative RT-PCR on cortical extracts 24 h after cerebral hypoxia-ischemia (HI) on P3 rats inducing (A) TNF-α and (B) IL-6 genes. Both sham groups (Sham-Iso and Sham-Lf) are shown despite being similar. Values are mean ± SEM, *$P < 0.05$, **$P < 0.01$, ***$P < 0.001$.

ing a variety of substrates associated with apoptotic cascades such as BAD and caspase-9. HI induced a decrease in the phosphorylated (active) form of AKT (P-AKT), which was significantly less under Lf treatment (HI-Iso: 62 ± 4%; HI-Lf: 77 ± 4%) (Fig. 6).

Discussion

The present study shows that multimodal NMR techniques providing metabolic, macro- and microstructural information allow characterization of brain damage and an accurate assessment of the neuroprotective effects of Lf nutritional supplementation during lactation. This study shows that Lf given to lactating dams as a nutritional supplement reduces damage resulting from HI injury in P3 rat pups.
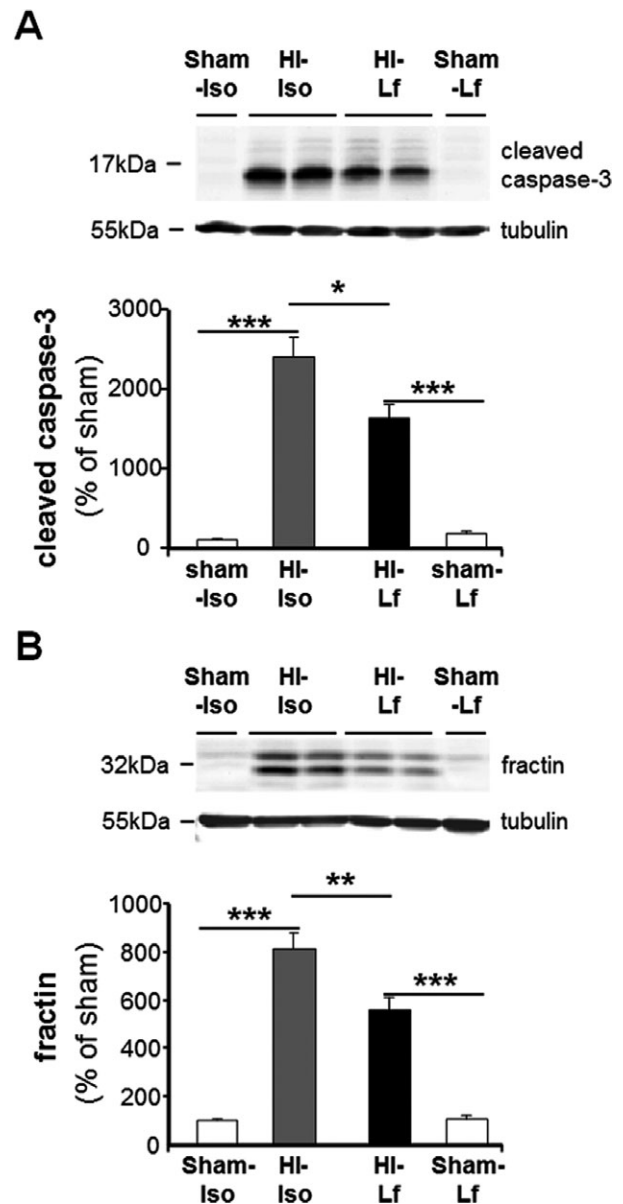

Figure 5. Lactoferrin treatment decreased activation of caspase-3. Representative immunoblots and the corresponding quantifications of cleaved caspase-3 (A) and fractin (B) demonstrating an activation of caspase-3 24 h after hypoxia-ischemia (HI) reduced by lactoferrin (Lf) treatment. Both sham groups (Sham-Iso and Sham-Lf) are shown despite being similar. Values are mean ± SEM and are expressed as a percentage of the Sham-Iso operated-animal value, *$P < 0.05$, **$P < 0.01$, ***$P < 0.001$.

T$_2$W MRI has previously been used to detect the presence of cerebral edema and assess its temporal evolution in the present model.[31] Five hours after HI, the injury was already clearly visible in the ipsilateral cortex as a hyperintense signal on the T$_2$W images due to edema presence. The edema was no longer visible at P25 but
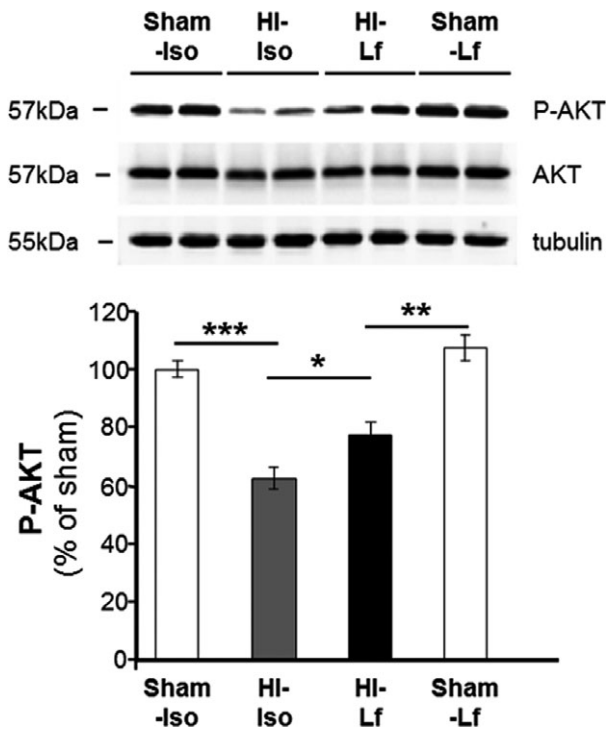
Figure 6. HI-induced AKT deactivation is less under lactoferrin treatment. Representative immunoblots and the corresponding quantifications of active phosphorylated AKT (P-AKT) and pan-AKT showing a dephosphorylation of AKT 24 h after hypoxia-ischemia (HI) reduced by lactoferrin (Lf) treatment. Both sham groups (Sham-Iso and Sham-Lf) are shown despite being similar. Values are mean ± SEM and are expressed as a percentage of the Sham-Iso operated-animal value, *$P < 0.05$, **$P < 0.01$, ***$P < 0.001$.

cortical damage appeared as a clear cortical dissymmetry. Maternal nutritional supplementation with Lf first reduced the extent of cortical injury 5 h post-HI as depicted by a reduced percentage of injured cortex at P3. Moreover, it preserved cortical development, as shown by a reduced cortical loss at P25. The evolution of the cortical lesion was similar in both HI-Iso and HI-Lf groups as shown by similar correlation coefficients between the percentage of injured cortex at P3 and cortical loss at P25 and similar *R*-values between the two groups. These results suggest that providing Lf through lactation reduces the severity of the initial brain damage (acute phase), resulting in a decreased lesion size at long term. It should be noticed that the percentage of rats injured per litter (i.e., showing an ipsilateral cortical hypersignal T_2 or an astrocytosis) was similar between the two groups and that Lf neuroprotection appears to be more efficient in females than males as indicated by reductions in the percentage of injured cortex at P3 and in cortical loss at P25.

^{1}H-MRS is a noninvasive method used to identify neurochemical changes induced in physiological and pathological conditions. ^{1}H-MRS showed that Lf treatment reduced the HI-induced alterations of the cortical neurochemical profile persisting at P25. Compared to Sham rats, only [NAA] was decreased in the Lf-treated rats, whereas a significant decrease in not only [NAA] but also [GABA] and Taurine as well as a significant increase in [NAAG] were observed in the lesion area of the HI-Iso group. NAA is assumed to be a marker of both neuronal death and/or of neuronal suffering.[51] Despite the neuroprotective effect of Lf in terms of lesion extent, the decrease in [NAA], measured in a very small volume of damaged area, indicated the presence of neuronal loss and/or dysfunction in both HI-Iso and HI-Lf groups still present 22 days post-insult. Since NAA is a precursor of NAAG, NAA could have been used to produce NAAG and the NAA decrease would then be related to the elevation of [NAAG] observed after HI even though this increase was not significant in Lf-treated rats. Moreover, NAAG has been shown to modulate neurotransmission[52] as an agonist of the metabotropic glutamate receptor mGluR3.[53, 54] Interestingly the HI-Iso group showed persistent altered neurotransmission in the damaged area reflected here by a significant decrease in inhibitory neurotransmitters (Taurine and GABA) which was not present in the HI-Lf group.

DTI provides microstructural data on the brain. HI insult leads to acute alterations in the developing cortex with long-term micro-architectural alterations that are reflected by changes in cortical DTI-derived parameters.[29,30] Here, we showed that the HI-Iso group presented reduced diffusivity values compared to both the Sham and the HI-Lf groups 22 days post-injury. In this HI model a substantial glial scar is present in the damaged cortex and remains in the long term accompanied by disruption of neuronal and axonal architecture.[29,30,55] The reduced diffusivities represent a modification of the microstructure in the injured cortical area of the non-treated animals which may be related to an astrogliotic reaction. DTI assessment provided evidence for partial recovery of cortical architecture in Lf-treated rats 22 days after injury. Cortical diffusivity values of the Lf-supplemented group were not significantly different from the Sham group, demonstrating a beneficial effect of Lf in protecting the cortical microstructure.

In very immature brains, the developing white matter is particularly vulnerable to HI injury.[12, 56] We previously demonstrated that, in this P3 moderate HI model, long-term myelination deficits occurred mainly in the intracortical white matter more than in white matter tracts.[30] Nevertheless, DTI-derived parameter alterations in the corpus callosum and the EC have already been observed

in this model.[43] Our results confirm our previous study with altered diffusivities and FA in the corpus callosum and EC for the HI-Iso group compared to Sham at P25.[43] The predominant decrease in axial diffusivity was responsible for the FA reduction. The axial diffusivity decrease may be related to axonal damages/misalignment[32] and altered myelination[34] but an inverse correlation between axial diffusivity and axon diameter has also been shown.[57] As such, the decrease in axial diffusivity could be related to larger axonal diameters and/or axonal damage/misalignments rather than myelination deficits. Whereas Lf supplementation had a clear positive effect on the EC as shown for the cortex with restored FA and diffusivity values, Lf did not preserve the structural organization of the corpus callosum at P25, showing reduced FA and abnormal diffusivity values.

Lodygensky et al.[38] recently showed that the phase contrast (the frequency shift observed between gray and white matter on phase images) was correlated to the degree of myelination during mouse brain development. Furthermore, the phase contrast can also be modified by other compounds influencing the local magnetic susceptibility such as axonal density.[39] In the EC, the frequency shift of HI-Lf and Sham groups are similar and lower than the HI-Iso group, matching the diffusion results and the preservation of the EC by Lf treatment. On the other hand, the corpus callosum seems to be compromised even in the Lf group as depicted by frequency shift values. Both these results are consistent with the DTI data and allow PCI to be used as a complement to DTI to further investigate axonal and myelination changes. It is important to notice that Lf binds iron which is a strong modulator of phase contrast but no difference was observed in Sham rats between those supplemented with Iso or with Lf.

The neuroprotective effect of Lf nutritional supplementation, shown here by a combination of NMR techniques, could be explained by the anti-inflammatory properties of Lf.[5,58,59] Indeed, the early reduction in the transcription of two proinflammatory cytokine genes, TNF-α and IL-6, known to be overexpressed in the immature rat brain after HI,[60–62] indicates reduced inflammatory reaction by Lf. Increased expression of both TNF-α and IL-6 have been detected in preterm neonates with periventricular leukomalacia[63] and represent a major source of brain inflammation that could be reduced by Lf. Despite some positive effects on neurons,[64,65] neuroinflammation is mainly involved in HI-induced cell death.[66] Different anti-inflammatory strategies have been shown to provide neuroprotection in models of perinatal HI injury.[67–69] The anti-inflammatory properties of Lf are thus possible causes of the neuroprotection. HI also strongly induces apoptotic mechanisms in the immature brain.[70–73] The anti-inflammatory properties of Lf may contribute to its antiapoptotic action[61,74] revealed here by reduced activation of caspase-3 and the related production of fractin in Lf-treated rat pups 24 h after HI. Interestingly, fractin has been shown to be present in the brains of preterms with periventricular leukomalacia.[75] The cleavage of actin into fractin may be not only an apoptotic marker but also a functional player in the apoptotic pathway.[76] The protective role of Lf may also be mediated by its ability to maintain the level of P-AKT higher after HI. In fact, the AKT pathway has prosurvival/antiapoptotic activities and its deactivation (dephosphorylation) is known to be involved in several cell death conditions including excitotoxicity and HI.[77–79] These results suggest that Lf can reduce brain damage after HI injury in the P3 rat by acting on at least two of the major injury pathways in the developing brain, namely inflammation and apoptosis. In addition, two other well-known properties of Lf, its antioxidant and iron-chelating powers, could also participate to reduce oxidative or iron-related mediators of the acute phase of HI injury.[80,81] Moreover, as the Lf treatment was started on the day of birth and HI was performed 3 days later, a preventive effect of Lf is probably involved.

Conclusion

These results show great promise in the field of neonatology and for the care of premature newborns. In addition to Lf's known actions of delaying preterm delivery,[13–15] preventing neonatal sepsis and necrotizing enterocolitis,[59] we have here demonstrated in a preclinical HI model of preterm brain damage that Lf can also protect the preterm brain against HI injury. This adds to prior studies showing that Lf has the potential to reduce altered brain development induced by intrauterine growth restriction.[16] An important feature of this study is that Lf is given to the dams during the lactation period from P0. Thus, to translate these experimental conditions to clinical studies, lactoferrin should be administrated as a preventive treatment to mothers with premature labor and risk of preterm delivery and then, after delivery, as a supplement for newborn neuroprotection.

Acknowledgments

Author Contribution

Y. v. d. L., V. G., A. C., A. T., E. S., P. S. H., and S. V. S. designed the experiment, Y. v. d. L., V. G., A. C., A. T., and E. S. acquired and analyzed the data, Y. v. d. L., V. G., A. C., A. T., E. S., P. S. H., and S. V. S. wrote the paper.

Conflict of Interest

None.

References

1. Walker A. Breast milk as the gold standard for protective nutrients. J Pediatr 2010;156(2 suppl):S3–S7.
2. Isaacs EB, Fischl BR, Quinn BT, et al. Impact of breast milk on intelligence quotient, brain size, and white matter development. Pediatr Res 2010;67:357–362.
3. Metz-Boutigue MH, Jolles J, Mazurier J, et al. Human lactotransferrin: amino acid sequence and structural comparisons with other transferrins. Eur J Biochem 1984;17:659–676.
4. Belizy S, Nasarova IN, Procof'ev VN, et al. Changes in antioxidative properties of lactoferrin from women's milk during deamidation. Biochemistry 2001;66:576–580.
5. Garcia-Montoya IA, Cendon TS, Arevalo-Gallegos S, et al. Lactoferrin a multiple bioactive protein: an overview. Biochim Biophys Acta 2012;1820:226–236.
6. Legrand D. Lactoferrin, a key molecule in immune and inflammatory processes. Biochem Cell Biol 2012;90:252–268.
7. Maneva A, Taleva B, Maneva L. Lactoferrin-protector against oxidative stress and regulator of glycolysis in human erythrocytes. Z Naturforsch [C] 2003;58:256–262.
8. Orsi N. The antimicrobial activity of lactoferrin: current status and perspectives. Biometals 2004;17:189–196.
9. Raghuveer TS, McGuire EM, Martin SM, et al. Lactoferrin in the preterm infants' diet attenuates iron-induced oxidation products. Pediatr Res 2002;52:964–972.
10. Nagasawa T, Kiyosawa I, Kuwahara K. Amounts of lactoferrin in human colostrum and milk. J Dairy Sci 1972;55:1651–1659.
11. Manzoni P, Rinaldi M, Cattani S, et al. Bovine lactoferrin supplementation for prevention of late-onset sepsis in very low-birth-weight neonates: a randomized trial. JAMA 2009;302:1421–1428.
12. Back SA, Luo NL, Borenstein NS, et al. Late oligodendrocyte progenitors coincide with the developmental window of vulnerability for human perinatal white matter injury. J Neurosci 2001;21:1302–1312.
13. Hasegawa A, Otsuki K, Sasaki Y, et al. Preventive effect of recombinant human lactoferrin in a rabbit preterm delivery model. Am J Obstet Gynecol 2005;192:1038–1043.
14. Mitsuhashi Y, Otsuki K, Yoda A, et al. Effect of lactoferrin on lipopolysaccharide (LPS) induced preterm delivery in mice. Acta Obstet Gynecol Scand 2000;79:355–358.
15. Paesano R, Pietropaoli M, Berlutti F, et al. Bovine lactoferrin in preventing preterm delivery associated with sterile inflammation. Biochem Cell Biol 2012;90:468–475.
16. Somm E, Larvaron P, van de Looij Y, et al. Protective effects of maternal nutritional supplementation with lactoferrin on growth and brain metabolism. Pediatr Res 2014;75:51–61.
17. Legrand D, Pierce A, Elass E, et al. Lactoferrin structure and functions. Adv Exp Med Biol 2008;606:163–194.
18. Suzuki YA, Lopez V, Lonnerdal B. Mammalian lactoferrin receptors: structure and function. Cell Mol Life Sci 2005;62:2560–2575.
19. Ji B, Maeda J, Higuchi M, et al. Pharmacokinetics and brain uptake of lactoferrin in rats. Life Sci 2006;78:851–855.
20. Kamalinia G, Khodagholi F, Atyabi F, et al. Enhanced brain delivery of deferasirox-lactoferrin conjugates for iron chelation therapy in neurodegenerative disorders: in vitro and in vivo studies. Mol Pharm 2013;10:4418–4431.
21. Liu Z, Jiang M, Kang T, et al. Lactoferrin-modified PEG-co-PCL nanoparticles for enhanced brain delivery of NAP peptide following intranasal administration. Biomaterials 2013;34:3870–3881.
22. Qian ZM, Wang Q. Expression of iron transport proteins and excessive iron accumulation in the brain in neurodegenerative disorders. Brain Res Brain Res Rev 1998;27:257–267.
23. Fillebeen C, Dexter D, Mitchell V, et al. Lactoferrin is synthesized by mouse brain tissue and its expression is enhanced after MPTP treatment. Adv Exp Med Biol 1998;443:293–300.
24. Kawamata T, Tooyama I, Yamada T, et al. Lactotransferrin immunocytochemistry in Alzheimer and normal human brain. Am J Pathol 1993;142:1574–1585.
25. Wang L, Sato H, Zhao S, et al. Deposition of lactoferrin in fibrillar-type senile plaques in the brains of transgenic mouse models of Alzheimer's disease. Neurosci Lett 2010;13:164–167.
26. Rousseau E, Michel PP, Hirsch EC. The iron-binding protein lactoferrin protects vulnerable dopamine neurons from degeneration by preserving mitochondrial calcium homeostasis. Mol Pharmacol 2013;84:888–898.
27. Volpe JJ. Brain injury in premature infants: a complex amalgam of destructive and developmental disturbances. Lancet Neurol 2009;8:110–124.
28. Sizonenko SV, Camm EJ, Garbow JR, et al. Developmental changes and injury induced disruption of the radial organization of the cortex in the immature rat brain revealed by in vivo diffusion tensor MRI. Cereb Cortex 2007;17:2609–2617.

29. Sizonenko SV, Kiss JZ, Inder T, et al. Distinctive neuropathologic alterations in the deep layers of the parietal cortex after moderate ischemic-hypoxic injury in the P3 immature rat brain. Pediatr Res 2005;57:865–872.

30. Sizonenko SV, Sirimanne E, Mayall Y, et al. Selective cortical alteration after hypoxic-ischemic injury in the very immature rat brain. Pediatr Res 2003;54:263–269.

31. van de Looij Y, Chatagner A, Huppi PS, et al. Longitudinal MR assessment of hypoxic ischemic injury in the immature rat brain. Magn Reson Med 2011;65:305–312.

32. van de Looij Y, Mauconduit F, Beaumont M, et al. Diffusion tensor imaging of diffuse axonal injury in a rat brain trauma model. NMR Biomed 2012;25:93–103.

33. Obenaus A, Ashwal S. Magnetic resonance imaging in cerebral ischemia: focus on neonates. Neuropharmacology 2008;55:271–280.

34. Favrais G, van de Looij Y, Fleiss B, et al. Systemic inflammation disrupts the developmental program of white matter. Ann Neurol 2011;70:550–565.

35. van de Looij Y, Lodygensky GA, Dean J, et al. High-field diffusion tensor imaging characterization of cerebral white matter injury in lipopolysaccharide-exposed fetal sheep. Pediatr Res 2012;72:285–292.

36. van Velthoven CT, van de Looij Y, Kavelaars A, et al. Mesenchymal stem cells restore cortical rewiring after neonatal ischemia in mice. Ann Neurol 2012;71:785–796.

37. Marques JP, Maddage R, Mlynarik V, et al. On the origin of the MR image phase contrast: an in vivo MR microscopy study of the rat brain at 14.1 T. NeuroImage 2009;46:345–352.

38. Lodygensky GA, Marques JP, Maddage R, et al. In vivo assessment of myelination by phase imaging at high magnetic field. NeuroImage 2012;59:1979–1987.

39. Wharton S, Bowtell R. Effects of white matter microstructure on phase and susceptibility maps. Magn Reson Med 2014; (doi 10.1002/mrm.25189).

40. Manzoni P, Meyer M, Stolfi I, et al. Bovine lactoferrin supplementation for prevention of necrotizing enterocolitis in very-low-birth-weight neonates: a randomized clinical trial. Early Human Dev 2014;90(suppl 1):S60–S65.

41. Ochoa TJ, Pezo A, Cruz K, et al. Clinical studies of lactoferrin in children. Biochem Cell Biol 2012;90:457–467.

42. Paesano R, Pacifici E, Benedetti S, et al. Safety and efficacy of lactoferrin versus ferrous sulphate in curing iron deficiency and iron deficiency anaemia in hereditary thrombophilia pregnant women: an interventional study. Biometals 2014;27:999–1006.

43. van de Looij Y, Chatagner A, Quairiaux C, et al. Multi-modal assessment of long-term erythropoietin treatment after neonatal hypoxic-ischemic injury in rat brain. PLoS One 2014;9:e95643.

44. Gruetter R, Tkac I. Field mapping without reference scan using asymmetric echo-planar techniques. Magn Reson Med 2000;43:319–323.

45. van de Looij Y, Kunz N, Huppi P, et al. Diffusion tensor echo planar imaging using surface coil transceiver with a semiadiabatic RF pulse sequence at 14.1T. Magn Reson Med 2011;65:732–737.

46. Hasan KM, Parker DL, Alexander AL. Comparison of gradient encoding schemes for diffusion-tensor MRI. J Magn Reson Imaging 2001;13:769–780.

47. Rivière D, Régis J, Cointepas Y, et al. A freely available Anatomist/BrainVISA package for structural morphometry of the cortical sulci. NeuroImage 2003;19:934.

48. Brehmer F, Bendix I, Prager S, et al. Interaction of inflammation and hyperoxia in a rat model of neonatal white matter damage. PLoS One 2012;7:e49023.

49. Sizonenko SV, Camm EJ, Dayer A, et al. Glial responses to neonatal hypoxic-ischemic injury in the rat cerebral cortex. Int J Dev Neurosci 2008;26:37–45.

50. Kamemori N, Takeuchi T, Sugiyama A, et al. Trans-endothelial and trans-epithelial transfer of lactoferrin into the brain through BBB and BCSFB in adult rats. J Vet Med Sci 2008;70:313–315.

51. Lei H, Berthet C, Hirt L, et al. Evolution of the neurochemical profile after transient focal cerebral ischemia in the mouse brain. J Cereb Blood Flow Metab 2009;29:811–819.

52. Neale JH, Olszewski RT, Zuo D, et al. Advances in understanding the peptide neurotransmitter NAAG and appearance of a new member of the NAAG neuropeptide family. J Neurochem 2011;118:490–498.

53. Wroblewska B, Santi MR, Neale JH. N-acetylaspartylglutamate activates cyclic AMP-coupled metabotropic glutamate receptors in cerebellar astrocytes. Glia 1998;24:172–179.

54. Wroblewska B, Wroblewski JT, Pshenichkin S, et al. N-acetylaspartylglutamate selectively activates mGluR3 receptors in transfected cells. J Neurochem 1997;69:174–181.

55. Dean JM, McClendon E, Hansen K, et al. Prenatal cerebral ischemia disrupts MRI-defined cortical microstructure through disturbances in neuronal arborization. Sci Transl Med 2013;5:168ra7.

56. Back SA, Han BH, Luo NL, et al. Selective vulnerability of late oligodendrocyte progenitors to hypoxia-ischemia. J Neurosci 2002;22:455–463.

57. Barazany D, Basser PJ, Assaf Y. In vivo measurement of axon diameter distribution in the corpus callosum of rat brain. Brain 2009;132(Pt 5):1210–1220.

58. Chatterton DE, Nguyen DN, Bering SB, et al. Anti-inflammatory mechanisms of bioactive milk proteins in the intestine of newborns. Int J Biochem Cell Biol 2013;45:1730–1747.

59. Lingappan K, Arunachalam A, Pammi M. Lactoferrin and the newborn: current perspectives. Expert Rev Anti Infect Ther 2013;11:695–707.

60. Hagberg H, Gilland E, Bona E, et al. Enhanced expression of interleukin (IL)-1 and IL-6 messenger RNA and bioactive protein after hypoxia-ischemia in neonatal rats. Pediatr Res 1996 Oct;40:603–609.

61. Li SJ, Liu W, Wang JL, et al. The role of TNF-alpha, IL-6, IL-10, and GDNF in neuronal apoptosis in neonatal rat with hypoxic-ischemic encephalopathy. Eur Rev Med Pharmacol Sci 2014;18:905–909.

62. Szaflarski J, Burtrum D, Silverstein FS. Cerebral hypoxia-ischemia stimulates cytokine gene expression in perinatal rats. Stroke 1995;26:1093–1100.

63. Yoon BH, Romero R, Kim CJ, et al. High expression of tumor necrosis factor-alpha and interleukin-6 in periventricular leukomalacia. Am J Obstet Gynecol 1997;177:406–411.

64. Lambertsen KL, Clausen BH, Babcock AA, et al. Microglia protect neurons against ischemia by synthesis of tumor necrosis factor. J Neurosci 2009;29:1319–1330.

65. Suzuki S, Tanaka K, Suzuki N. Ambivalent aspects of interleukin-6 in cerebral ischemia: inflammatory versus neurotrophic aspects. J Cereb Blood Flow Metab 2009;29:464–479.

66. Leonardo CC, Pennypacker KR. Neuroinflammation and MMPs: potential therapeutic targets in neonatal hypoxic-ischemic injury. J Neuroinflammation 2009;6:13.

67. Carty ML, Wixey JA, Reinebrant HE, et al. Ibuprofen inhibits neuroinflammation and attenuates white matter damage following hypoxia-ischemia in the immature rodent brain. Brain Res 2011;1402:9–19.

68. Martin D, Chinookoswong N, Miller G. The interleukin-1 receptor antagonist (rhIL-1ra) protects against cerebral infarction in a rat model of hypoxia-ischemia. Exp Neurol 1994;130:362–367.

69. Wixey JA, Reinebrant HE, Spencer SJ, et al. Efficacy of post-insult minocycline administration to alter long-term hypoxia-ischemia-induced damage to the serotonergic system in the immature rat brain. Neuroscience 2011;182:184–192.

70. Nakajima W, Ishida A, Lange MS, et al. Apoptosis has a prolonged role in the neurodegeneration after hypoxic ischemia in the newborn rat. J Neurosci 2000;20:7994–8004.

71. Northington FJ, Ferriero DM, Graham EM, et al. Early neurodegeneration after hypoxia-ischemia in neonatal rat is necrosis while delayed neuronal death is Apoptosis. Neurobiol Dis 2001;8:207–219.

72. Stadlin A, James A, Fiscus R, et al. Development of a postnatal 3-day-old rat model of mild hypoxic-ischemic brain injury. Brain Res 2003;993:101–110.

73. Zhu C, Wang X, Xu F, et al. The influence of age on apoptotic and other mechanisms of cell death after cerebral hypoxia-ischemia. Cell Death Differ 2005;12:162–176.

74. Wang Y, Cao M, Liu A, et al. Changes of inflammatory cytokines and neurotrophins emphasized their roles in hypoxic-ischemic brain damage. Int J Neurosci 2013;123:191–195.

75. Haynes RL, Billiards SS, Borenstein NS, et al. Diffuse axonal injury in periventricular leukomalacia as determined by apoptotic marker fractin. Pediatr Res 2008;63:656–661.

76. Schulz R, Vogel T, Mashima T, et al. Involvement of Fractin in TGF-beta-induced apoptosis in oligodendroglial progenitor cells. Glia 2009;57:1619–1629.

77. Luo HR, Hattori H, Hossain MA, et al. Akt as a mediator of cell death. Proc Natl Acad Sci USA 2003;100:11712–11717.

78. Mullonkal CJ, Toledo-Pereyra LH. Akt in ischemia and reperfusion. J Invest Surg 2007;20:195–203.

79. van den Tweel ER, Kavelaars A, Lombardi MS, et al. Bilateral molecular changes in a neonatal rat model of unilateral hypoxic-ischemic brain damage. Pediatr Res 2006;59:434–439.

80. Ferriero DM. Neonatal brain injury. N Engl J Med 2004;351:1985–1995.

81. Vogel HJ. Lactoferrin, a bird's eye view. Biochem Cell Biol 2012;90:233–244.